

Development of chloropyromorphite coatings for lead water pipes

Jeremy D. Hopwood,^a Roger J. Davey,^{*a} Merfyn O. Jones,^b Robin G. Pritchard,^b Peter T. Cardew^c and Ann Booth^d^aDepartment of Chemical Engineering, UMIST, Manchester, UK M60 1QD^bDepartment of Chemistry, UMIST, Manchester, UK M60 1QD^cUnited Utilities, Lingley Mere Business Park, Great Sankey, Warrington, UK WA5 3LP^dLGC-North West, The Heath, Runcorn Cheshire, UK WA7 4DQ

Received 17th December 2001, Accepted 9th April 2002

First published as an Advance Article on the web 30th April 2002

Formation of inorganic barrier coatings on lead water pipes might be an attractive option for water companies wishing to reduce lead levels in drinking water. This paper concerns the treatment of such pipes with aqueous solutions containing oxidant together with sources of phosphate and chloride to generate coatings of the highly insoluble lead mineral chloropyromorphite, $Pb_5(PO_4)_3Cl$ by simultaneous oxidation and precipitation. SEM, TEM, XRD and overnight leaching tests were used to characterise the structure and performance of the coatings. The impact of the choice of oxidant on the coating morphology and barrier properties is explored. Strategies for further refinement of the coatings *via* improved process control and morphological modification are discussed.

Introduction

Lead is a cumulative poison, readily exchanging for calcium in the body¹ and in the past was a serious problem for homes supplied by acidic soft waters. Until 1970, it was standard practice for homes in the UK to be connected to the water mains *via* a lead pipe. Although copper or plastic piping is now used, many homes still contain the original lead pipe, which lies underground, is not visible and in large houses can be up to 40 m long. The oxidative corrosion of the pipe surface, by dissolved oxygen and disinfectants such as hypochlorite, is then the principal source of ionic lead entering domestic tap water. Dissolved anions, such as carbonate, react with lead ions to form a mineral scale and the lead level in the water is then limited by the solubility of these corrosion products. Today, parameters such as pH, alkalinity, hardness *etc* are optimised at the water treatment works to minimise this solubilisation and ensure safe use. Following a review of water quality and taking into account health concerns the European Union² has revised the current limit of $50 \mu\text{g l}^{-1}$ ($0.024 \mu\text{M}$) down to $10 \mu\text{g l}^{-1}$ ($0.005 \mu\text{M}$) which will become a statutory requirement by 2013.

Mineral scale formation provides a mechanism by which lead is removed from solution and in principle the maximum dissolved concentration of lead in tap water should be a function of the mineral solubility. Thus, if this scale comprises the least soluble, most supersaturated, lead mineral phase then the lead level in the water should be minimised. Tap waters that promote the formation of low solubility phases are therefore preferred over those that do not. Waters that fall into the latter category can be altered at the treatment works. Solubility models, based on ion speciation calculations, have been developed to assist with this process.^{3–7}

For most tap waters, the least soluble lead mineral phases are the carbonates: cerussite $PbCO_3$, hydrocerussite $Pb_3(OH)_2(CO_3)_2$ and plumbonacrite $Pb_{10}O(CO_3)_6(OH)_6$. Addition of phosphate ($1.5\text{--}3 \mu\text{g l}^{-1}$, $16\text{--}32 \mu\text{M}$) causes lead phosphates: tetraplumbite orthophosphate hydrate $Pb_4(OH)_2(PO_4)_2$, hydroxyppyromorphite $Pb_5(PO_4)_3OH$, tertiary lead orthophosphate $Pb_3(PO_4)_2$ and chloropyromorphite $Pb_5(PO_4)_3Cl$ to become the least soluble lead mineral phases (Fig. 1). For this reason phosphate dosing at the treatment works has proved very successful in reducing lead levels and is now a key part of

plumbosolvency control measures taken to achieve compliance in the UK.^{8–11}

Of the phosphate phases, chloropyromorphite is the most interesting since according to its solubility this mineral should reduce lead levels to below $1 \mu\text{g l}^{-1}$ (Fig. 1), well below the $10 \mu\text{g l}^{-1}$ limit. In practice, however, such low levels are not observed, implying that either chloropyromorphite does not form or that its growth is slow. In the work reported here we explore the possibility that the $10 \mu\text{g l}^{-1}$ limit may be achieved by treating the pipes *in situ* in such a way as to create a protective coating of chloropyromorphite. Not only would chloropyromorphite not dissolve but it might continue to grow when later treated with phosphate dosed tap water. In a coating process, based on that used by the automotive industry^{12–14} we used potassium peroxydiphosphate ($K_4P_2O_8$), hydrogen peroxide, sodium hypochlorite, hydrogen ions and dissolved

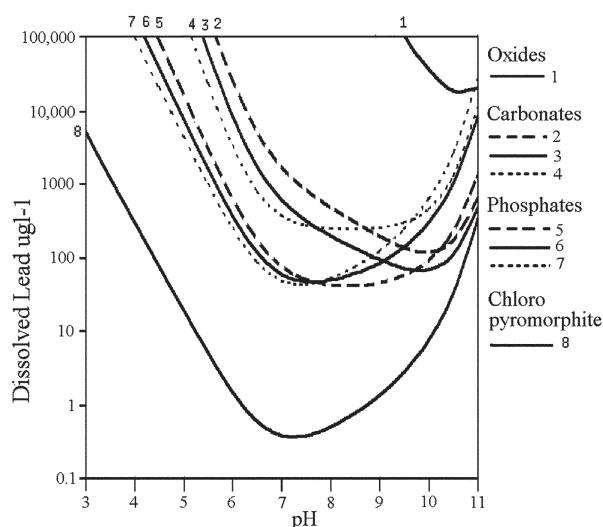


Fig. 1 Solubilities of lead compounds in phosphate dosed Manchester City (soft, low conductivity) tap water. 1: Lead oxide (α and β), 2: plumbonacrite, 3: hydrocerussite, 4: cerussite, 5: tetraplumbite orthophosphate hydrate, 6: hydroxyppyromorphite, 7: tertiary lead orthophosphate.^{4,6,7}

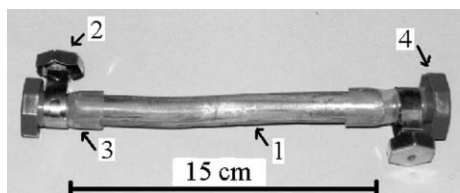


Fig. 2 Piece of lead pipe. 1: Lead pipe, 2: screw clip, 3: silicone tubing, 4: plastic T-shaped cap.

oxygen (water saturated at room temperature) as the oxidising agents to release lead ions which would then react with added phosphate and chloride to produce chloropyromorphite as a coating on the inside of a pipe (Table 1).

Materials

New lead piping of internal and external diameter 1.08 and 1.67 cm and length 15 cm was supplied by United Utilities (Fig. 2). Sodium chloride, nitric acid, hydrochloric acid, sodium hydroxide and disodium hydrogen phosphate were of analytical grade and obtained from Aldrich and Fluka. Tetrapotassium peroxydiphosphate (KAPER[®]), 96% w/w,

Table 1 Standard electrochemical potentials

Equilibrium	E^0/V
$Pb^{2+} + 2e^- \rightleftharpoons Pb_{(s)}$	-0.126
$O_2 + 4H^+ + 4e^- \rightleftharpoons 2H_2O$ (acidic)	+1.229
$O_2 + 2H_2O + 4e^- \rightleftharpoons 4OH^-$ (alkaline)	+0.401
$2H^+ + 2e^- \rightleftharpoons H_2$	Zero
$P_2O_8^{4-} + 2e^- \rightleftharpoons 2PO_4^{3-}$	+2.07
$H_2O_2 + 2H^+ + 2e^- \rightleftharpoons 2H_2O$	+1.776
$O_2 + 2H^+ + 2e^- \rightleftharpoons 2H_2O_2$	+0.695
$2HClO + 2H^+ + 2e^- \rightleftharpoons Cl_2 + 2H_2O$ (acidic)	+1.59
$ClO^- + H_2O + 2e^- \rightleftharpoons Cl^- + 2OH^-$ (alkaline)	+0.89

Table 2 Composition of Manchester City tap water

Species	Conc./ μM	Species	Conc./ μM
$O_2(g)$	≈ 300	SO_4^{2-}	29
CO_3^{2-}	430	K^+	19
Cl^-	270	PO_4^{3-}	14
Ca^{2+}	250	F^-	2
Na^+	200	Fe^{3+} (max.)	2–24
Mg^{2+}	49	pH	8.4
NO_3^-	45	Ionic strength	1.2 mM

Table 3 Coating treatments, their initial compositions and corresponding lead leach values. Experiments 1–8 were pH adjusted with HCl (0.1 M) and experiments 9–16 were adjusted with HNO_3 (1.0 M)

Expt	$[PO_4^{3-}]/mM$	$[NaCl]/mM$	Added oxidant	$[Oxidant]/mM$	pH	Lead leach value (average)/ $\mu g\ l^{-1}$	Coating
1	0.02	2.5	$K_4P_2O_8$	0.25	8.0	570	A1
2	0.02	25.0	$K_4P_2O_8$	0.25	8.0	480	A1
3	0.02	2.5	$K_4P_2O_8$	0.25	3.0	37,500	B1
4	0.02	25.0	$K_4P_2O_8$	0.25	3.0	50,000	B1
5	0.2	2.4	$K_4P_2O_8$	2.4	7.6	800	A1
6	0.2	24.0	$K_4P_2O_8$	2.4	7.6	400	A1
7	0.2	2.4	$K_4P_2O_8$	2.4	3.0	670	A2
8	0.2	24.0	$K_4P_2O_8$	2.4	3.0	490	A2
9	0.5	2.6	H_2O_2	290.0	3.0	1150	— ^a
10	3.0	1.0	NaOCl	0.5	7.0	270	— ^a
11	30.0	10.0	NaOCl	5.0	7.0	600	— ^a
12	3.0	1.0	—	—	3.0	540	A3
13	3.0	1.0	—	—	7.0	210	A4
14	30.0	10.0	—	—	7.0	1000	— ^a
15	30.0	10.0	—	—	3.0	1450	— ^a
16	0.5	2.6	—	—	3.0	59,500	B2, B3

^aIndicates coatings that were not characterised.

was donated by FMC Corporation, Active Oxidants Division and included 3.5% w/w dipotassium hydrogen phosphate, 0.5% w/w potassium nitrate and possibly 0.3% w/w potassium fluoride (analysis by FMC). Hydrogen peroxide solution (27.5% w/w in water) and sodium hypochlorite solution (1.8 M NaOCl, 2.2 M NaCl and 0.7 M NaOH) were purchased from Aldrich. Analytical grade water was single distilled and passed through an ion exchange resin. Tap water was taken from the Manchester City supply zone (typical analysis Table 2).

Methods

Preparation of lead pipes

Thirty-two pieces of pipe, two repeats per experiment, were prepared. Each was carefully trimmed to a length of 15 cm using either a lead pipe cutter or a stainless steel Stanley knife blade. To ensure that only the insides of the pipes made contact with the coating solution, to avoid contaminating the leaching experiments and to make the pipes safer to handle the ends and external surfaces of the pipe were varnished using Eukitt (purchased from Agar).

Preparation of coating solutions

The coating solutions were prepared using the oxidant, phosphate and sodium chloride concentrations shown in Table 3. Buffer diagrams were used to determine the amounts of strong acid for experiments 1–8 and a modified ion speciation computer program IONPRODUCT¹⁴ was used to do likewise for experiments 9–16.

Coating procedure

Each coating experiment was carried out by continuously circulating the coating solution (volume 2 litres) through two pieces of lead pipe in series, *via* a reservoir and a peristaltic pump (Watson and Marlow 601C). The lead pipes were held in a vertical position and the flow rate through the pipes was 25 ml s^{-1} (0.26 m s^{-1}), corresponding to a Reynolds number of 3210 (onset of turbulent flow is >2000). High density polyethylene containers were used as reservoirs for the solutions. Experiments were run for three hours after which time the pipes were removed.

Lead leach experiments

After treatment, pipes were emptied of solution and sealed at one end using a piece of silicone rubber tubing, a plastic

T-shaped stopper and a metal screw clip (Fig. 2). Separate tests on the tubing and stopper showed that they did not leach lead. The pipes were then filled with mains tap water and left standing for 3 minutes before being emptied and refilled a further five times, so as to remove all traces of the treatment solution. After this they were filled once more, sealed at both ends and left standing at room temperature for 24 hours. The pipes were then unsealed and the leach solutions poured into high-density polyethylene (HDPE) plastic bottles. These were used as they adsorbed the least amount of lead from solution. In separate tests low density plastic, Pyrex and glass bottles were found to be strong adsorbers.

The concentration of lead was measured using a Palintest SA-1000 stripping voltammetry kit (ex. Palintest, Gateshead, Tyne and Wear, UK) with a measurable range of $2\text{--}100\ \mu\text{g l}^{-1}$ ($0.01\text{--}0.5\ \mu\text{M}$). Most solutions had lead levels above this range and were therefore diluted. Dilutions of 1, 10, 100 and 500 were made in quick succession prior to measurement, a Palintest stabilising pill being added to each dilution.

Analysis of coatings

Pipes for microscopy and X-ray powder diffraction were emptied of leach solution and gently rinsed in distilled water for a couple of minutes after which some were drained vertically onto lint free, water absorbent, paper and air dried, whilst others were cut open and placed face down onto lint free paper for more rapid drying.

Scanning electron microscopy was performed using a Hitachi S-520 instrument operated at $5\text{--}30\ \text{KeV}$. Samples were glued to aluminium stubs and electrical contact between the stub and sample made with either carbon or silver conducting paste. The samples were then sputter coated with gold for $1\frac{1}{2}$ minutes, allowed to cool and then sputtered for a further $1\frac{1}{2}$ minutes with a Polaron E 5000 water cooled sputter coater. It was very important to ensure that the samples were kept cool during sputtering, as high local temperatures on the sample surface could cause degradation due to the low melting point of lead and its compounds, causing the surface to go black.

X-ray powder diffraction patterns were recorded on a Scintag Inc. diffractometer (Cu source, $\lambda = 1.5406\ \text{\AA}$), which was designed solely for flat samples. This meant that the lead pipe pieces had to be flattened. Almost flat surfaces were achieved on cut sections of pipe by pressing down on their outside surface using a heavy metal plate. In this way flattened pieces of pipe of length and width 2.5 and $1.8\ \text{cm}$ respectively were produced. The absence of a perfectly flat surface meant that the peak positions were sometimes shifted by up to 0.4 degrees in the direction of lower 2θ values. However, the degree of shift could be readily ascertained from movement of the lead metal peaks. Identification of lead compounds was achieved by overlaying and comparing peaks within a pattern with patterns of known lead compounds from the JCPDS cards (numbers: chloropyromorphite – 19-701; massicot – 38-1477; litharge 5-561; hydroxypyromorphite 24-586). This was performed using Microsoft Excel. In the case of chloropyromorphite its spectrum is very similar to that for hydroxypyromorphite $\text{Pb}_5(\text{PO}_3)_3\text{OH}$. The two materials have been distinguished by counting the number of peaks between $45\text{--}47$ degrees 2θ . In this region hydroxypyromorphite has two peaks (Fig. 6f) and chloropyromorphite has three (Fig. 6g). Using this criterion only chloropyromorphite was observed in this study. The two repeat samples showed identical coating behaviour in all the experiments.

Preparation of synthetic chloropyromorphite

In order to have reference material for comparison with the coatings chloropyromorphite was prepared synthetically. In

the first preparation, a lead solution containing $1.0\ \text{mM PbCl}_2$ and $0.61\ \text{mM HCl}$ was mixed with an equal volume of a phosphate solution containing $1.0\ \text{mM Na}_2\text{HPO}_4$ and $0.61\ \text{mM HCl}$. The IONPRODUCT computer programme¹⁵ (adapted for lead using published ion-pair and solubility data⁴) predicted the initial and final pH values, on mixing, to be pH 4 and pH 3.2 respectively and the chloropyromorphite supersaturation to be $S = 159$. The second preparation was undertaken at a higher initial pH. A lead solution containing $1.0\ \text{mM PbCl}_2$ was mixed with an equal volume of a phosphate solution containing $1.0\ \text{mM Na}_2\text{HPO}_4$, $1.2\ \text{mM NaCl}$ and $0.45\ \text{mM NaOH}$. In this case the initial and final pH values, on mixing, were predicted to be pH 7 and pH 4 respectively and the chloropyromorphite supersaturation to be $S = 10,000$. The products were analysed by X-ray powder diffraction and TEM.

Results

Lead leach data

Lead leach values for coated pipes exposed to Manchester City tap water for 24 hours, under stagnant conditions, ranged from 210 to $59,500\ \mu\text{g l}^{-1}$ (Table 3). An identical test for five untreated lead pipes produced values between 2000 and $5400\ \mu\text{g l}^{-1}$ (mean $3460\ \mu\text{g l}^{-1}$ and standard deviation, $\sigma_n - 1$, $1493\ \mu\text{g l}^{-1}$ respectively). In general, the effect of the coating process was to reduce the lead leach values, although there were some notable exceptions where a large increase was observed.

Classification

We have classified the coatings according to their performance. Good coatings, denoted **type A**, gave lead leach values $< 1000\ \mu\text{g l}^{-1}$. Poor coatings, denoted **type B**, gave lead leach values $> 35,000\ \mu\text{g l}^{-1}$. Pipes that gave lead leach values in between were not classified.

SEM and XRD analysis of type A coatings revealed four morphological types (Fig. 3), denoted here as type A1, A2, A3 and A4. SEM and XRD analysis of type B coatings revealed three morphological types (Fig. 4) denoted here as type B1, B2 and B3.

Structure and composition of coatings

Uncoated pipes. Lead pipes are manufactured by an extrusion process in which pressurised molten lead is forced upwards through a water cooled cylindrical mould. The inner and outer surfaces of the pipe tarnish in the hot mould (reacting with oxygen *etc*) and emerge dull grey.

The extrusion process was very evident on the untreated pipes. SEM analysis showed parts of the surface to be heavily marked by draw-lines, which ran parallel to the long axis of the pipe. In many instances deep crevices were observed. Other parts of the pipe were much smoother with less pronounced draw-lines and metal grains were visible.

XRD analysis of the surface (Fig. 3) showed litharge ($\alpha\text{-PbO}$) to be the main component of the air formed metal oxide film. A small amount of hydrocerussite ($\text{Pb}_3(\text{CO}_3)_2(\text{OH})_2$) and an unidentified phase were also present.

Peroxydiphosphate initiated coatings. Treatment with the peroxydiphosphate containing solutions produced three types of coatings: A1, A2 and B1.

Type A1 coatings were formed under slightly alkaline conditions (pH $7.6\text{--}8.0$), at moderate and low oxidant concentration ($\text{P}_2\text{O}_8^{4-} = 0.25\text{--}2.4\ \text{mM}$). Visually and under the optical microscope, the coated pipes looked identical to untreated pipes. However, SEM analysis revealed a uniform coating of small rounded particles (diameter $0.05\text{--}0.2\ \mu\text{m}$, Fig. 3a). The only exception to the uniformity of the coating occurred at lead

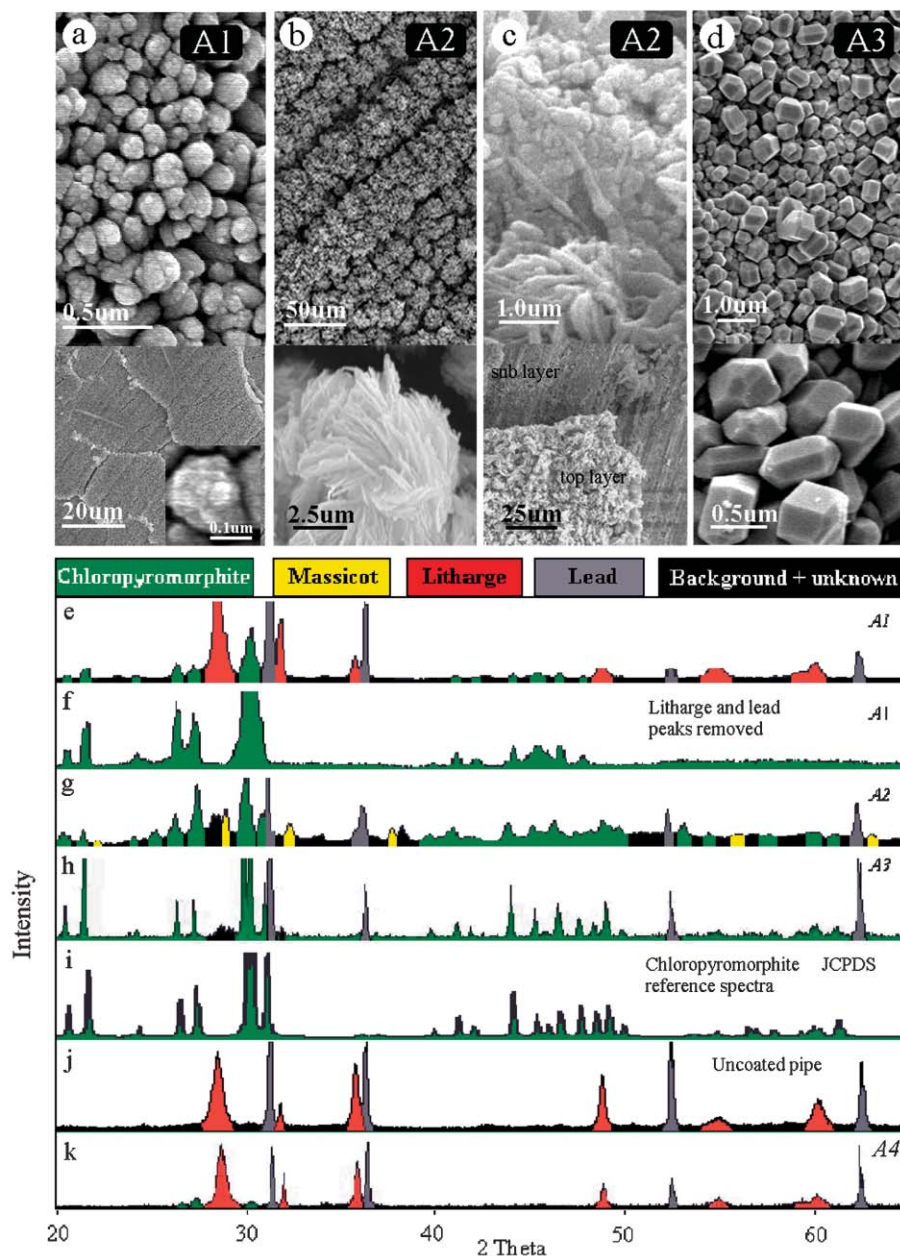


Fig. 3 SEM micrographs and powder XRD patterns of good coatings. Lead leach values $< 1000 \mu\text{g l}^{-1}$. (a, e and f) A1 coatings; (b, c and g) A2 coatings; (d and h) A3 coatings; (k) A4 coatings. The JCPDS spectrum for chloropyromorphite (i) and the spectrum for an uncoated pipe (j) are also shown.

grain boundaries and on some draw-lines, where bunching of particles and crevices was observed. The XRD spectra of the type A1 coating revealed it to comprise litharge ($\alpha\text{-PbO}$) and chloropyromorphite ($\text{Pb}_5(\text{PO}_4)_3\text{Cl}$). The pattern for litharge was very similar to that observed on the untreated pipe, suggesting that litharge remained fixed to the pipe during growth of the type A1 coating. Hence, the rounded particles and therefore the coating are assumed to be chloropyromorphite.

Type A2 coatings were formed under combined conditions of low pH and moderate oxidant concentration ($\text{pH} = 3.0$, $\text{P}_2\text{O}_8^{4-} = 2.4 \text{ mM}$). Visible to the naked eye, the coatings were initially white, turning yellow on drying and once dry the coating had a tendency to flake off. SEM (Fig. 3b) revealed closely packed aggregates (diameter $5 \mu\text{m}$) of flake-like particles (thickness $0.15 \mu\text{m}$). Parts of the coating appeared to replicate the topography of the underlying metal structure so that it was easy to tell where the draw-lines had been. Images of coating fragments implied that the thickness of the coating was

approximately $10 \mu\text{m}$. Areas where the coating had broken away revealed a substructure of irregular shaped particles (Fig. 3c). XRD showed the type A2 coating to be predominantly chloropyromorphite ($\text{Pb}_5(\text{PO}_4)_3\text{Cl}$) with massicot ($\beta\text{-PbO}$) as a minor component.

Type B1 coatings were formed under combined conditions of low pH and low oxidant concentration ($\text{pH} = 3.0$, $\text{P}_2\text{O}_8^{4-} = 0.25 \text{ mM}$). The pipes were initially white but became yellow on drying. It was difficult to resolve structural details by optical microscopy but SEM (Fig. 4a) revealed an open network of large plates (diameter approx. $40 \mu\text{m}$). These were intergrown with another type of particle, which may have been plates viewed end on or needles (thickness $0.7 \mu\text{m}$). SEM analysis of areas not containing plates (Fig. 4b) revealed a sublayer of much smaller rounded and rod-like particles (diameter $0.2\text{--}0.8 \mu\text{m}$). XRD revealed massicot ($\beta\text{-PbO}$) and to a lesser extent chloropyromorphite ($\text{Pb}_5(\text{PO}_4)_3\text{Cl}$) as well as a trace of an unknown phase. The irregular plates were most probably crystals of massicot which is a yellow mineral and when grown

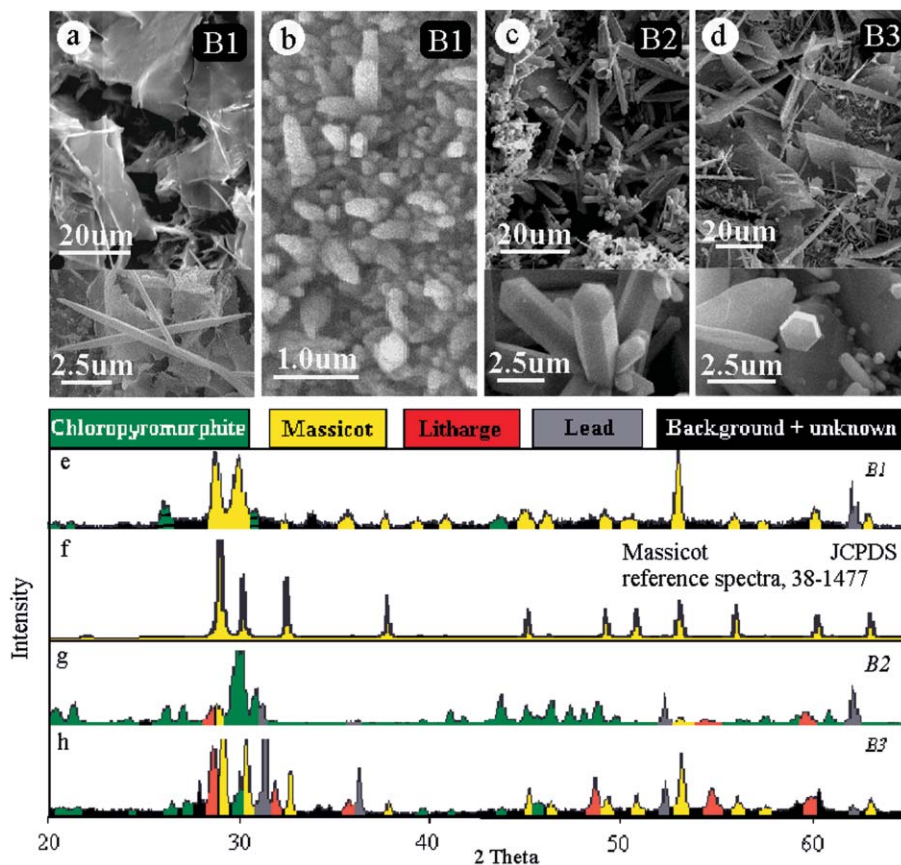


Fig. 4 SEM micrographs and powder XRD patterns of poor coatings. Lead leach values $> 35,000 \mu\text{g l}^{-1}$. (a, b, e) B1 coatings; (c and g) B2 coatings; (d and h) B3 coatings. The JCPDS spectrum for massicot is also shown.

synthetically exhibits a plate-like morphology. Whether or not the small rounded and rod-shaped particles were crystals of chloropyromorphite remains uncertain.

Hydrogen peroxide initiated coatings. Treatment with acidified hydrogen peroxide solution (1% w/w, pH 3.0, 0.5 mM PO_4^{3-}) did produce chloropyromorphite but the coatings were not adherent and the chloropyromorphite became suspended in solution producing a cloudy white precipitate. Analysis of the suspended material (XRD and SEM images not shown) revealed oval shaped chloropyromorphite particles (diameter 0.2–1 μm).

Experiments in which small pieces of pipe were submerged in treatment solution and observed using an optical microscope revealed streams of gas bubbles emanating from the pipe surface. These bubbles were probably oxygen gas liberated from partial decomposition of hydrogen peroxide and it is likely that entrapment followed by release of gas would break up any coating.

Sodium hypochlorite initiated coatings. Treatment with sodium hypochlorite ($\text{NaOCl} = 0.5\text{--}5 \text{ mM}$) at pH 7.0 produced lead leach values $< 1000 \mu\text{g l}^{-1}$. Although a positive result, the values were similar to those produced in the absence of hypochlorite (Expts 13 and 14, Table 3), suggesting that hypochlorite was not the active ingredient in the process.

Visually, the treated pipes looked identical to untreated pipes and so any coating must have been thin. SEM and XRD analyses were not undertaken.

Hydrogen ions and dissolved oxygen initiated coatings. Treatment with water open to the atmosphere at neutral and acidic pH, in the presence of phosphate and chloride, produced four types of coating: A3, A4, B2 and B3.

Type A3 coatings grew at low pH and moderate phosphate

and chloride concentrations (pH = 3.0, $\text{PO}_4^{3-} = 3 \text{ mM}$, $\text{Cl}^- = 1 \text{ mM}$). The coating was white and clearly visible to the naked eye. SEM analysis (Fig. 3d) revealed a highly uniform structure comprising well faceted particles (diameter 0.2–1.0 μm). Other more elongated particles were also observed, which were located in areas running parallel to the long axis of the pipe, rather like the original draw lines. XRD analysis showed the coatings to be predominantly chloropyromorphite.

Type A4 coatings (not shown) formed at neutral pH and moderate phosphate and chloride concentrations (pH = 7.0, $\text{PO}_4^{3-} = 3 \text{ mM}$, $\text{Cl}^- = 1 \text{ mM}$). Visually, the treated pipes looked identical to untreated pipes and so any coating must have been thin. SEM was not undertaken. The XRD spectra exhibited prominent peaks for litharge and lead metal, similar to those for untreated pipes. However, chloropyromorphite was also identified as a minor component.

Type B2 coatings (Fig. 4c) grew under combined conditions of low pH, low phosphate and moderate chloride concentrations (pH = 3.0, $\text{PO}_4^{3-} = 0.5 \text{ mM}$, $\text{Cl}^- = 2.6 \text{ mM}$) and were white and friable. SEM analysis revealed a loose open network of well defined rods that were hexagonal in cross-section (length 2–20 μm). XRD analysis showed chloropyromorphite to be the predominant phase with litharge as a minor component.

Type B3 coatings (Fig. 4d) were formed under the same conditions as type B2 except that the coatings were dried more gradually by draining. These coatings were yellow and not white. SEM revealed a mass of large intergrown plates (diameter 20–50 μm , thickness 4–7 μm). Hexagonal rod-shaped crystals were also present but were much less obvious than those observed on the type B2 coatings. The XRD spectra revealed mostly massicot ($\beta\text{-PbO}$), presumably corresponding to the large intergrown plates. Chloropyromorphite was a minor component as were litharge ($\alpha\text{-PbO}$) and lead metal.

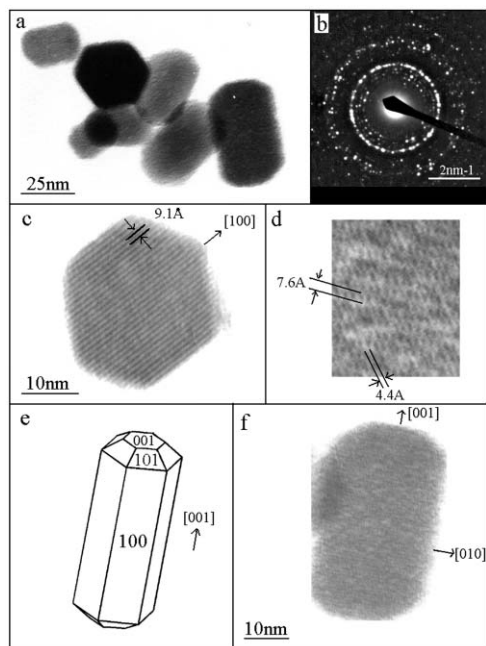


Fig. 5 TEM and powder electron diffraction analysis of synthetic chloropyromorphite crystals together with a sketch showing the most likely morphology. The image in (d) is a high resolution image of the crystal in (f).

Synthetic chloropyromorphite

Mixing of lead, phosphate and chloride (0.5, 0.5 and 0.61 mM) under acid conditions (pH 4) resulted in the formation of a white precipitate. Analysis by TEM (Fig. 5) showed the precipitate to consist of elongated hexagonal crystals (size 0.01–0.04 μm). Well defined lattice fringes of d -spacing 9.1, 7.6 and 4.4 \AA were observed that could be indexed to the (001), (100) and {111} chloropyromorphite crystal planes, implying that the crystals were elongated along their c -axes with (001) top and bottom faces and {101} and {100} side faces (Fig. 5e). This is the form most commonly associated with geological

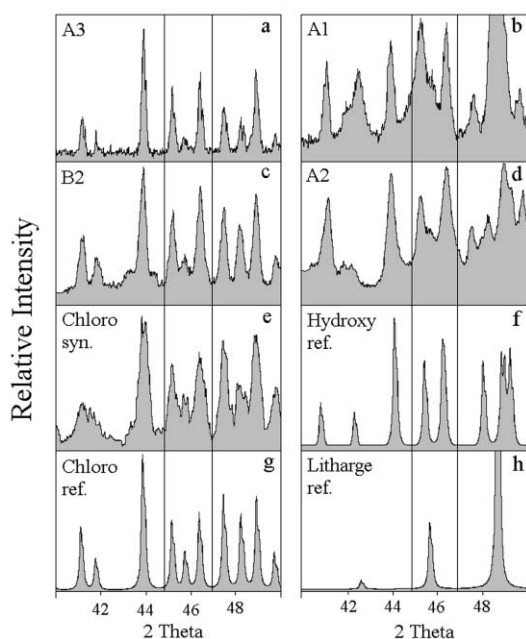


Fig. 6 Comparison of XRD spectra: (a) type A3 coatings; (b) type A1 coatings; (c) type B2 coatings; and (d) type A2 coatings; (e) synthetic chloropyromorphite (preparation 2); (f) hydroxypyromorphite JCPDS; (g) chloropyromorphite JCPDS; and (h) litharge JCPDS.

chloropyromorphite¹⁶ and was also the morphology observed in the type B2 and A3 coatings.

Mixing of lead, phosphate and chloride (0.5, 0.5 and 0.6 mM) under neutral conditions (pH 7) also produced a white precipitate. Analysis by powder XRD confirmed the presence of chloropyromorphite (Fig. 6e).

Discussion

Peroxydiphosphate was used because it offered the attraction of incorporating both oxidant and phosphate source into a single reactant, thereby simplifying an eventual application process. A simple calculation shows that, in the range of concentrations utilised, complete reaction of the peroxydiphosphate would have led to coatings of thicknesses in the range 6–120 μm dependent on their porosity. In practice, the observed coatings were thinner, falling in the range 2 μm (type A1)–25 μm (type A2), implying that the reactant did not supply the expected level of phosphate and hence that it is significantly less reactive than anticipated.¹⁷ Given this situation it seems likely that phosphate was supplied by the background phosphate present in the peroxydiphosphate samples (3.5% w/w) and that the lead ions were supplied either by dissolution of the existing air-formed α -lead oxide (litharge) film or by release of lead from oxygen and hydrogen ion corrosion. In the type A1 coatings the X-ray intensities of the litharge peaks are similar to those on untreated pipes, suggesting that the chloropyromorphite coatings must have formed by dissolution and re-precipitation of the outer surface of the litharge film with the bulk of the litharge remaining intact. The presence of litharge, albeit beneath a chloropyromorphite layer, may not be a good prospect as it is a semiconductor and therefore may speed up corrosion. That the source of phosphate was background phosphate was further supported by the similarity of type A1 coatings to layers found on lead pipes exposed to phosphate dosed tap water.¹⁸

Under the acid conditions used for coatings A2 and B1 litharge is very soluble (Fig. 1, pH 3.0) and so its dissolution was complete. The reduction in pH also led to increased oxidation by protons and dissolved oxygen, giving rise to thicker coatings. Given that peroxydiphosphate was not active as an oxidant the differences in behaviour of A2 and B1 must be due to the level of background phosphate (0.2 vs 0.02 mM K_2HPO_4) with there being insufficient in the B1 case to precipitate the flux of lead leaving the pipe. In this latter case the appearance of the soluble β -lead oxide (massicot) is thought to be an artefact forming as a result of lead release during washing and leaching, the lead pipe being poorly protected on account of acid exposure. The solubility of this oxide is approximately $50,000 \mu\text{g l}^{-1} \text{Pb}$ (Fig. 1), consistent with the leach values and its yellow colour would also explain the yellowing of the pipes on drying.

The use of other oxidants, hydrogen peroxide and sodium hypochlorite, together with phosphate added as Na_2HPO_4 did not really give any significant improvements. Oxygen bubbles from the peroxide negated any positive effects (compare experiments 9 and 16, Table 3) due to the disruption it caused to the coating integrity. Sodium hypochlorite appeared to have little effect at all (experiments 10, 11, 13 and 14, Table 3) on the thickness or efficacy of the coating. It seems reasonable to conclude that the oxidising agents peroxydiphosphate, hydrogen peroxide and sodium hypochlorite played at best a minor role in the development of the chloropyromorphite coatings and that the important oxidants were oxygen and hydrogen ions.

The performance of the coatings generated at different pH values and phosphate concentrations is summarised below in Table 4. Treatment at pH 7.0 and 3.0 mM phosphate gave rise to thin type A4 coatings of chloropyromorphite and

Table 4 Performance of coatings as a function of pH and mM phosphate concentration

PO ₄ ³⁻ pH	0.5	3	30
7		Good	Intermediate
3	Poor	Good	Intermediate

the corresponding lead leach values were low (210 µg l⁻¹). Increasing the phosphate concentration to 30.0 mM also produced thin coatings but these were less effective at preventing lead leaching (1000 µg l⁻¹). A similar trend was observed for treatments undertaken at pH 3.0: coatings produced at 30.0 mM phosphate exhibited higher leach values (1450 µg l⁻¹) than those produced at 3.0 mM phosphate (540 µg l⁻¹, type A3). However, the opposite trend occurred on further decreasing the phosphate concentration so that at 0.5 mM phosphate the lead leach values were again higher (59,500 µg l⁻¹, type B2, B3 coatings).

The explanations for the growth of the coatings are similar to those already described. The good A4 coatings produced at pH 7 and 3.0 mM phosphate probably grew in the same way as the type A1 coatings in the peroxydiphosphate experiments. That is, by dissolution of the outer surface of litharge (α-PbO) followed by precipitation of a thin chloropyromorphite layer. Likewise, the poor B2/B3 coatings grown at pH 3 and 0.5 mM phosphate probably grew in a similar manner to the B1 coatings, by complete dissolution of the litharge layer followed by hydrogen ion and oxygen oxidative attack and depletion of an insufficient concentration of phosphate ions. As before, the resulting chloropyromorphite coatings offered very poor protection and slow draining of the pipes, after the leach experiments, generated massicot (B3 coatings). Sufficient phosphate (3.0 mM) at pH 3.0 produced the good A3 coatings. The coatings that gave intermediate lead leach values were all produced at high phosphate concentrations (30.0 mM), suggesting that too much phosphate produced ultra thin coatings, which were unstable when later exposed to tap water.

It is clear from the data that it is possible to create a coating which corresponds structurally to chloropyromorphite and yet despite its low aqueous solubility is unable to provide a good barrier to lead leaching. For example, the lowest lead leach values recorded were in the range 185–400 µg l⁻¹, which is four to ten times greater than the current European Union recommended limit of 50 µg l⁻¹ and over 200 times greater than the equilibrium value for the dissolution of chloropyromorphite. One important cause of this discrepancy is likely to relate to the morphology of the coating and the extent to which it seals the underlying lead surface. Good, low porosity, coatings are likely to be those in which the crystals are well interconnected and have plate-like morphologies oriented parallel to the metal surface. In this work a variety of chloropyromorphite crystal morphologies were observed, as discussed below, yielding both dense and open coatings.

The experiments at pH 3.0 (coatings A3 and B2) gave rise to well faceted prismatic crystals as did the synthetic experiments at pH = 4.0. In fact the B2 crystals were morphologically similar to the synthetic crystals (Fig. 5), both containing a six-fold axis and elongated along the *c*-axis. The B2 crystals were all orientated with their long axes at different angles to the pipe surface. This together with the low number density meant that the coating was ineffectual as a barrier. The A3 crystals appear to form the most coherent coating in this study. Like the B2 crystals they were randomly orientated with respect to the pipe surface but their number density was very high and their low aspect ratio meant that they were closely packed and formed a uniform coating over large areas of pipe surface. The peroxydiphosphate experiments at pH 7.6–8.0 and pH 3.0

(coatings A1, A2 and B1) gave rise to rounded and irregular shaped chloropyromorphite particles. In the case of the type A1 coatings it is not possible to say whether the lack of well formed crystals did or did not impact on coating performance: that the particles were closely packed may have been more important. Comparing the reaction conditions for the rounded A1 particles with those for the faceted crystals (type A3 and B2) suggests that the chloropyromorphite morphology might be pH and phosphate dependent, low pH and moderate phosphate concentration yielding well faceted crystals and neutral pH and low phosphate concentration being associated with rounded particles.¹⁹

A future development strategy would include both improved monitoring of the lead, phosphate and chloride concentrations during the coating process and morphological control of the precipitated crystals. In the former case avoiding depletion of phosphate and chloride during the reaction might further enhance the performance of the type A3 coatings. In the latter case process modification to yield a coating of plate-like, preferentially oriented crystals stacked parallel to the metal surface may create an improved barrier.

Finally, it is worth noting here that lead is also an important issue in the remediation of contaminated land and immobilisation of lead in 'brown field' sites by transformation of high solubility salts to low solubility pyromorphites is also being explored.^{20,21} A lead metal/mineral interface is also of great importance in the manufacture of lead-acid automotive batteries.²² This work may also be useful to other studies on the development of inorganic barrier coatings.

Acknowledgement

The authors would like to thank United Utilities, UK for funding this work.

References

- 1 World Health Organization, *Guidelines for drinking water quality: Recommendations*, 1993, 2nd Edn, Vol. 1, pp. 49–50.
- 2 The Council of the European Union, *Quality of water intended for human consumption*, 1998, Council Directive 98/83/EC.
- 3 D. Marani, G. Macchi and M. Pagano, *Water Res.*, 1995, **29**, 1085.
- 4 M. R. Schock, *Journal of American Water Works Association*, 1980, **72**, 695.
- 5 P. Taylor and V. J. Lopata, *Can. J. Chem.*, 1984, **62**, 395.
- 6 I. Sheiham and P. J. Jackson, *J. Inst. Water Eng. Sci.*, 1981, **35**, 491.
- 7 P. T. Cardew, *Water Res.*, 2000, **34**, 2241.
- 8 J. H. Colling, B. T. Croll, A. E. Whincup and C. Harward, *J. Inst. Water Environ. Manage.*, 1992, **6**, 259.
- 9 Water and Waste Treatment magazine: *Lead costs cut by chemicals*, Faversham House Group, London, 2000, (May), p. 6.
- 10 B. P. Boffardi and A. M. Sherbondy, *Corrosion*, 1991, **47**, 966.
- 11 *Lead Control Strategies*, American Water Works Association (AWWA) Research Foundation, Denver, 1990.
- 12 W. Rausch, *The phosphating of metals*, Finishing Publications, Teddington, Middlesex, UK, 1990.
- 13 K. F. Ang, S. Turgoose and G. E. Thompson, *Trans. Inst. Met. Finish.*, 1991, **69**, 58.
- 14 D. Weng, P. Jokiel, A. Uebles and H. Boehni, *Surf. Coat. Technol.*, 1996, **88**, 147.
- 15 R. P. Shellis, *Comput. Appl. Biosci.*, 1988, **3**, 373.
- 16 J. D. Dana and E. S. Dana, *Dana's system of mineralogy*, Seventh edition, 1944/1951, Vol. I/II, John Wiley, New York.
- 17 W. P. Griffith, R. D. Powell and A. C. Skapski, *Polyhedron*, 1988, **7**, 1305.
- 18 J. H. Colling, P. A. E. Whincup and C. R. Hayes, *J. Inst. Water Environ. Manage.*, 1987, **1**, 263.
- 19 E. C. Moreno, M. Kresak and A. Gaffar, *J. Colloid Interface Sci.*, 1994, **168**, 173.
- 20 Q. Y. Ma, S. J. Traina, T. J. Logan and J. A. Ryan, *Environ. Sci. Technol.*, 1993, **27**, 1803.
- 21 P. Zhang and J. A. Ryan, *Environ. Sci. Technol.*, 1999, **33**, 625.
- 22 R. Dell, *Chem. Br.*, 2000, **36**, 34.